Journal of Hazardous Materials 160 (2008) 94–99

Contents lists available at ScienceDirect

Journal of Hazardous Materials

journal homepage: www.elsevier.com/locate/jhazmat

Viscosity of high-alcohol content fuel blends with water: Subsurface contaminant transport implications

Kenneth Y. Lee*

Department of Civil and Environmental Engineering, University of Massachusetts Lowell, 1 University Avenue, Lowell, MA 01854, USA

ARTICLE INFO

Article history:
Received 5 November 2007
Received in revised form 30 January 2008
Accepted 25 February 2008
Available online 4 March 2008

Keywords:
Alternative fuels
Subsurface contamination
E85
M85
Viscosity

ABSTRACT

In the United States, a gasoline fuel blend with alcohol volume fractions of 85% or more is considered (among other fuels) an alternative fuel. As the popularity and usage of high-alcohol content gasoline fuel blends increase, subsurface contamination from these fuels will be of great environmental concern. An important parameter governing the movement of these contaminants in unsaturated porous media is the liquid viscosity. In this study, five sets of experiments are conducted to determine viscosity variations of (a) blends of 15% gasoline with various alcohol mixtures, and (b) mixtures of high-alcohol content gasoline fuel blends with various volume fractions of water. The three alcohols considered in this study are ethanol, methanol, and isopropanol. The viscosity of each liquid mixture is observed using a modified falling-ball viscometer.

1. Introduction

Under the United States Energy Policy Act of 1992 (EPAct), alcohols (e.g. ethanol and methanol), as well as blends of 85% or more of alcohol with gasoline, are considered (among other fuels) as alternative fuels. The M85 and E85 fuels, for example, are fuel blends containing (by volume) 85% methanol with 15% unleaded gasoline, and 85% ethanol with 15% unleaded gasoline, respectively. Currently, there are several automobile manufacturers producing flexible-fuel vehicles (FFV) capable of running on regular unleaded gasoline as well as on the E85 fuel. The E85 fuel can be purchased at selected fueling stations in numerous states.

Ethanol is mainly produced from corn in the United States [4]. Consequently, the availability and price of ethanol depends heavily on corn production, which can vary year to year depending on agricultural and economic conditions. The demand for ethanol is already high; as 10% ethanol is presently added to approximately one third of all the gasoline to fulfill oxygenate requirements for federal clean air programs [4]. As the popularity and usage of the E85 fuel increases, the demand for ethanol will amplify accordingly. One possible solution to alleviate the high ethanol demand is to consider a mixture of alcohols, such as a mixture of ethanol, methanol, and/or some other alcohols such as isopropanol (isopropyl alcohol), for the makeup of the required 85% alcohol volume in gasoline fuel blends. Unlike ethanol, methanol is normally produced from natural gas, and can be produced from coal or biomass crops [1].

It is anticipated that the frequency of accidental spills and underground storage tank leakage from high-alcohol content fuel blends will increase. After an aquifer is contaminated, it may take years of costly remediation to restore the subsurface to its original state. While there are abundant studies on subsurface contamination issues resulting from the release of petroleum fuels, there is relatively less research on contamination issues resulting from the release of alternative fuels, particularly on high-alcohol content gasoline blends. Alcohols such as ethanol, isopropanol, and methanol are independently miscible in both gasoline and water. As water is continuously added to a high-alcohol content gasoline fuel blend, the water is initially mixed with the fuel blend as a single-phase liquid. However, at water volume fractions past a threshold value, the alcohol–gasoline–water mixture partitions into a two-phase liquid–liquid system [6]. This threshold water volume fraction value depends on the type of alcohol and the gasoline composition. Consequently, as the leaked fuel blend migrates downward in the unsaturated zone and encounters moisture, the fuel blend will initially mix with the water increasing the overall contaminant volume. Ultimately, if the water volume fraction of the mixture exceeds the threshold value, the single-phase mixture will partition into a two-phase system.

The addition of water also changes the viscosity of the fuel mixture. Viscosity is an important parameter for contaminant transport in porous media [3]. In this study, five sets of experiments are conducted to determine viscosity variations of (a) blends of 15% gasoline with various alcohol mixtures, and (b) mixtures of

* Tel.: +1 978 934 2255.
E-mail addresses: kenneth_lee@uml.edu, leekennethy@gmail.com.

0304-3894/$ – see front matter © 2008 Elsevier B.V. All rights reserved.
doi:10.1016/j.jhazmat.2008.02.088

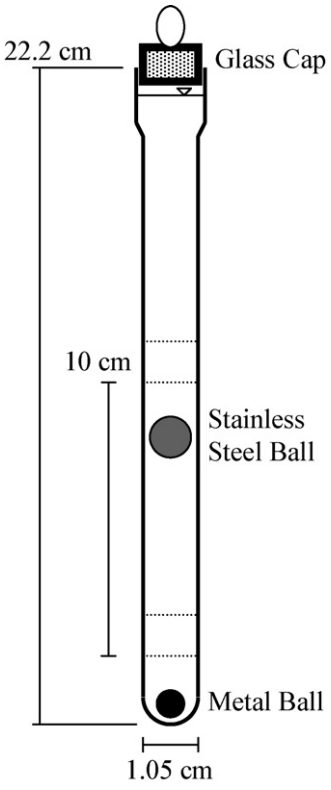

Fig. 1. Drawing of the modified falling-ball viscometer.

high-alcohol content fuel blends with various volume fractions of water. It should be noted that this study observed the viscosity variations of single-phase alcohol–gasoline–water liquid mixtures only. The viscosity of each mixture is determined using a modified commercially available falling-ball viscometer. A falling-ball viscometer consists basically of a glass tube and a spherical bead that is used as the falling ball. As the ball falls through a target liquid at its terminal velocity, the viscosity can be determined from measuring the time-of-descent for the ball to travel a fixed vertical distance down the glass tube. A falling-ball viscometer is suitable for viscosity measurement of Newtonians fluids, and should not be used for viscosity measurement of non-Newtonian fluids.

2. Materials and methods

Fig. 1 shows a drawing of the modified falling-ball viscometer (not drawn to scale). The glass tube has an outer diameter of 1.05 cm and a height of 22.2 cm, and is commercially available from Gilmont® Instruments (Barrington, IL, USA). The falling ball used in all viscosity experiments is a 0.635 cm (1/4 in.) diameter stainless steel (type 316) spherical ball also supplied by Gilmont® Instruments, and it has a density of 8.02 g/cm^3. The metal spherical ball, which is not supplied by Gilmont® Instruments, has a diameter of 0.5 cm and weights at 0.437 g. A glass cap is used to seal the glass tube after it is filled with the target liquid(s).

It is critical that the falling-ball viscometer be placed in an exact vertical position for accurate and reproducible experimental results [2]. To accomplish this task, an apparatus for holding and leveling the viscometer is constructed. Fig. 2 shows a drawing of the leveling apparatus. The top illustration is a plan view of the leveling apparatus and the bottom illustration is the front view. The leveling apparatus has a plastic post level (Johnson Level & Tool, Model #175) permanently attached to a wood base with three height-adjustable legs. A post level is generally used for proper installation of fence posts, and it contains three liquid-filled gas bubble levels; one in the vertical direction and the other two are in the horizontal direction 90° from each other. The viscometer is securely attached to the inner center of the level post using a rubber band. The viscometer is considered leveled when the gas bubble in each of the two horizontal liquid-filled levels is adjusted (by varying the height of each of the three legs) to the center of each level.

The metal ball (see Fig. 1) can be moved vertically upward and downward inside the glass tube by moving an external magnet. The metal ball serves two purposes. First, repeated vertical movement of the metal ball aids in the mixing of the liquid compounds inside the glass tube. Second, upward movement of the metal ball pushes the overlying stainless steel ball upward, thus allowing repeated time-of-descent measurements of the same liquid. For every time-of-descent measurement, the stainless steel ball is pushed upward (via the metal ball) to a height near the top of the glass tube (but below the fluid level), and then the external magnet is released causing both the metal ball and the stainless steel ball to fall downward. Due to its relatively smaller size, the metal ball falls downward at a much higher velocity than the stainless steel ball, thus reaching (and resting at) the bottom of the glass tube almost instantly.

As the stainless steel ball falls downward through a liquid (or a mixture of liquids), it accelerates due to gravity until it reaches a steady-state constant velocity. This constant velocity is known as the terminal velocity. At terminal velocity, the gravitational force exactly equals to the buoyant and kinetic forces acting on the falling ball. The terminal velocity for a vertically falling spherical ball in a tube, v_T, can be described by the following equation, which is derived from Stokes' solution [2]:

$$v_T = \frac{2}{9}\left(\frac{g(\rho_B - \rho_{FL})a^2}{\kappa\mu}\right) \quad (1)$$

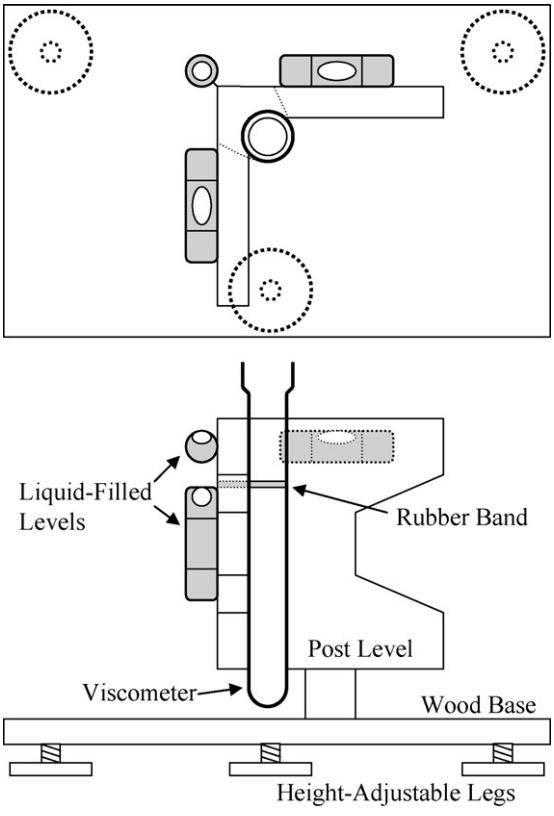

Fig. 2. Drawing of the viscometer leveling apparatus.

where g is the gravity, ρ_B the density of the falling ball, ρ_{FL} the density of the liquid or liquid mixture, a the radius of the falling ball, μ the liquid mixture viscosity (in centipoise, or cP) and κ is a correction factor to account for effects such as wall effects and inertial effects not presented in Stokes' original solution. Note that one centipoise is equal to one millipascal second (1 cP = 1 mPa s). The reader can refer to the work of Feng et al. [2] for analysis of the various factors affecting the accuracy and reproducibility of observed viscosity using a falling-ball viscometer.

The terminal velocity can be determined by observing the time it takes for the falling ball to travel a known vertical distance inside the viscometer. Eq. (1) can be rearranged to determine the liquid viscosity:

$$\mu = \left(\frac{2ga^2}{9\kappa L}\right)(\rho_B - \rho_{FL})t \quad (2)$$

where L is the vertical traveled distance of the falling ball and t is the time-of-descent for the falling ball to travel distance L. If L is a known fixed distance on the glass tube and the radius of the falling ball is also known, then the variables in the first parentheses of Eq. (2) can be replaced by an overall viscometer constant. Eq. (2) can be reduced to:

$$\mu = K(\rho_B - \rho_{FL})t \quad (3)$$

where K is the overall viscometer constant. For the falling-ball viscometer used in this study, Eq. (3) can be applied to determine the viscosity of a liquid mixture by measuring the time-of-descent for the stainless steel ball to travel a vertical distance of 10 cm (see Fig. 1). The overall viscometer constant K can be determined from Eq. (3) by measuring t for a standard liquid with known viscosity and density values.

For each viscosity experiment, the glass tube is filled with a pre-determined amount of target liquid(s) totaling 6.7 mL. Next, the metal ball is carefully inserted into the glass tube followed by the insertion of the stainless steel ball. A glass cap is then immediately placed on top of the glass tube to minimize volatilization. The glass tube is then securely attached to the leveling apparatus. The two horizontal liquid-filled gas bubble levels on the post level are checked for levelness. The three legs on the leveling apparatus are height-adjusted if necessary. If the target solution contains more than one liquids, the metal ball is moved up-and-down the glass tube numerous times to assure that the solution is well-mixed. The mixing process usually takes several minutes. Then the time-of-decent observations are conducted. A stopwatch is used to determine the falling ball descent time. The time-of-descent observation is repeated for the same solution until four consistent falling ball descent times are recorded. Note that these four falling ball descent times are used for liquid viscosity calculations. Next, the glass cap is removed and approximately 1 mL of solution is withdrawn from the glass tube using a 3 mL BD™ (Becton, Dickinson and Company, Franklin Lakes, New Jersey, USA) disposable syringe with 1.5 in. needle. The solution volume within the syringe is determined by reading the syringe markings. The weight of the solution inside the syringe is determined by the difference in syringe weight before and after fluid withdrawal. The density of the each target liquid mixture is approximated by dividing the syringe liquid mass by the syringe liquid volume.

3. Results and discussion

3.1. Determination of the overall viscometer constant

The overall viscometer constant using the stainless steel falling ball is obtained by observing the ball's time-of-descent through a liquid with known density and viscosity values. Eq. (3) can be rearranged to determine K:

$$K = \frac{\mu}{(\rho_B - \rho_{FL})t} \quad (4)$$

Table 1
Published density and viscosity values

Compound	CAS no.	Molecular formula	Density at 20 °C (kg/m^3)	Viscosity at 20 °C (cP)
Ethanol[a]	64-17-5	C_2H_6O	789.2	1.184
Methanol[a]	67-56-1	CH_4O	790.9	0.583
Isopropanol[b]	67-63-0	C_3H_8O	785	2.27
Water[c]	7732-18-5	H_2O	998.2	1.005

[a] Kumagai and Yokoyama [5].
[b] Material Safety Data Sheet (MSDS).
[c] Mays [8].

As noted earlier, the density of the stainless steel ball is 8.02 g/cm^3. Table 1 lists the published density and viscosity values of pure ethanol, methanol, isopropanol, and water at 20 °C (293.15 K). All alcohols used in this study are obtained from Fisher Scientific (www.fishersci.com). The denatured ethanol used in the study is of HPLC grade, the methanol is of HPLC grade, and the isopropanol is of laboratory grade. Using ethanol, the viscometer constant is determined as K = 0.17 cP cm^3/(g min). Using this K value, the observed viscosity value is 0.59 cP for methanol, 2.17 cP for isopropanol, and 1.02 cP for the distilled water used in this study. These experimentally derived viscosity values are consistent with published viscosity values listed in Table 1. Therefore, the value of K = 0.17 cP cm^3/(g min) is considered valid and used for all subsequent viscosity calculations. The regular unleaded gasoline (87 octane) used in this study is purchased from a gasoline station in Montgomery, West Virginia, USA. The density of this gasoline is determined as 0.765 g/mL, and the viscosity of this gasoline is observed as 0.39 cP. The synthetic E85 and M85 fuel blends used in this study are created by mixing solutions comprising of 15% gasoline with 85% ethanol, and 15% gasoline with 85% methanol, respectively. It should be noted that the viscosity (and composition) of gasoline varies from brand to brand and from location to location. Therefore, the resulting E85 or M85 fuel blend viscosity will also vary accordingly. It should also be noted that liquid viscosity is temperature dependent, and the temperature of the laboratory fluctuates minimally between 19 and 21 °C (292.15–294.15 K). However, this small temperature fluctuation should not significantly impact the experimental results.

3.2. Fuel blends comprising of gasoline and various volume fractions of ethanol and methanol

The first set of experiments is conducted to determine viscosity variations for fuel blends comprising of 15% regular unleaded gasoline and various volume fractions of ethanol and methanol. A total of 11 viscosity experiments are conducted and the results are plotted as circles in Fig. 3(a). Each circle represents the averaged viscosity value from four consistent experimentally derived viscosity values as described earlier. In Fig. 3(a), the top horizontal axis represents the ethanol volume fraction and the bottom horizontal axis represents the methanol volume fraction. It should be noted that in all figures, volume fractions are expressed as percentages. Also note that for each data point in this figure, the summation of the ethanol volume and the methanol volume is equal to 85% of the total solution volume. The first circle (at 0% methanol volume) indicates the observed averaged viscosity value for the E85 fuel (1.016 cP) and the last circle (at 85% methanol volume) indicates the observed averaged viscosity value for the M85 fuel (0.572 cP). The dotted lines represent the viscosity value of each indicated liquid,

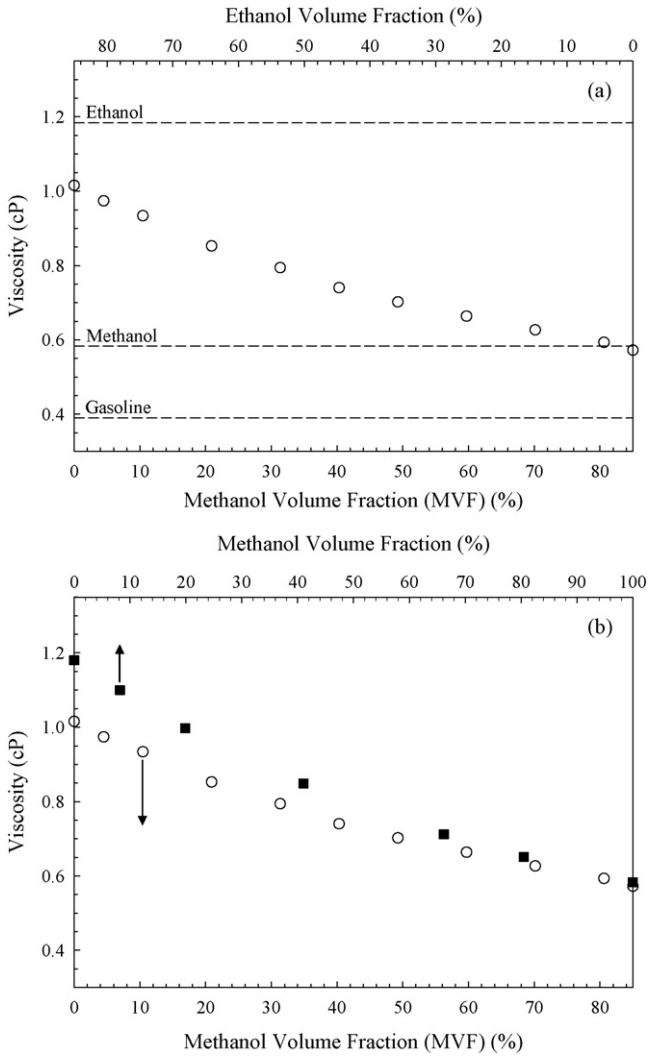

Fig. 3. (a) Observed viscosity variations for fuel blends comprising of 15% gasoline and various volume fractions of ethanol and methanol. (b) Comparison between the observed viscosity values of (a) and viscosity values presented by Kumagai and Yokoyama [5].

and these values are plotted in each figure to provide a comparison of each liquid mixture's observed viscosity against the viscosity of the various liquid components that made up the mixture. All experimentally derived averaged viscosity values presented in Figs. 3–7 are also listed in Table 2 along with 95% confidence intervals. The 95% confidence intervals are too small to be visible in the figures and thus are not plotted.

Fig. 3(b) shows a comparison between the experimentally derived viscosity values (circles) of Fig. 3(a) and published viscosity values (solid squares) for mixtures comprising of various volume fractions of ethanol and methanol only [5]. The bottom horizontal axis of Fig. 3(b) represents the methanol volume fraction for the data set presented in Fig. 3(a). The top horizontal axis represents the methanol volume fraction for the data set presented by Kumagai and Yokoyama [5], which was conducted at a temperature of 20 °C (293.15 K). Due to addition of gasoline, the scale of the bottom horizontal axis is different than the scale of the top horizontal axis. For example, the third circle in Fig. 3(b) (with an arrow pointing downward), represents the averaged observed viscosity value of a fuel blend containing 15% gasoline, 74.5% ethanol, and 10.5% methanol. The second solid square (with an arrow pointing upward) represents the viscosity value for a binary liquid mixture containing 91.8% ethanol and 8.2% methanol. Note that the two experimentally derived viscosity data sets show similar viscosity variations. However, the difference in viscosity value between ethanol and the E85 fuel is relatively larger than the difference in viscosity value between methanol and the M85 fuel.

3.3. Fuel blends comprising of gasoline and various volume fractions of ethanol and isopropanol

The second set of experiments is conducted to determine viscosity variations for fuel blends containing 15% regular unleaded gasoline and various volume fractions of ethanol and isopropanol. A total of 10 additional viscosity experiments are conducted and the results are listed in Table 2 and plotted as circles in Fig. 4. Again, the summation of the ethanol volume and the methanol volume for each data point is equal to 85% of the total solution volume, and the viscosity of isopropanol, ethanol, and gasoline are plotted as dotted lines. Note that isopropanol has relatively the highest viscosity among all three alcohols considered in this study. Therefore, the viscosity of the fuel mixture is expected (and experimentally shown) to increase as the volume fraction of isopropanol increases.

3.4. Mixtures of the E85 fuel with various volume fractions of water

The third set of experiments is conducted to determine viscosity variations for liquid mixtures comprising of the E85 fuel with various volume fractions of water. For the first viscosity experiment, a small-predetermined amount of water is added into the glass tube followed by the addition of the E85 fuel. The solution is then mixed using the metal ball, and checked visually for phase separation. If no phase separation is detected after several minutes, the solution is assumed to be a single-phase liquid and the time-of-descent observations are allowed to proceed according to the procedure described earlier. For each subsequent viscosity experi-

Table 2
Experimentally derived averaged viscosity values and corresponding 95% confidence intervals

Fig. 3		Fig. 4		Fig. 5		Fig. 6		Fig. 7	
MVF	Viscosity (cP)	IVF	Viscosity (cP)	WVF	Viscosity (cP)	WVF	Viscosity (cP)	WVF	Viscosity (cP)
0	$1.016 \pm 4.61 \times 10^{-3}$	0	$1.016 \pm 4.61 \times 10^{-3}$	0	$1.016 \pm 4.61 \times 10^{-3}$	0	$0.572 \pm 1.07 \times 10^{-3}$	0	$0.764 \pm 2.03 \times 10^{-3}$
4.5	$0.974 \pm 6.57 \times 10^{-4}$	4.5	$1.033 \pm 2.52 \times 10^{-3}$	3.0	$1.133 \pm 3.20 \times 10^{-3}$	3.0	$0.687 \pm 1.09 \times 10^{-3}$	3.0	$0.895 \pm 1.59 \times 10^{-3}$
10.5	$0.934 \pm 9.50 \times 10^{-4}$	10.5	$1.056 \pm 1.24 \times 10^{-3}$	6.0	$1.241 \pm 1.06 \times 10^{-2}$	4.5	$0.750 \pm 8.83 \times 10^{-4}$	6.0	$1.003 \pm 2.20 \times 10^{-3}$
20.9	$0.853 \pm 1.19 \times 10^{-3}$	20.9	$1.134 \pm 1.42 \times 10^{-3}$	9.0	$1.340 \pm 1.50 \times 10^{-2}$	6.0	$0.792 \pm 2.57 \times 10^{-3}$	9.0	$1.136 \pm 3.12 \times 10^{-3}$
31.3	$0.794 \pm 5.00 \times 10^{-4}$	31.3	$1.168 \pm 7.80 \times 10^{-3}$	11.9	$1.468 \pm 2.23 \times 10^{-2}$	7.5	$0.701 \pm 1.41 \times 10^{-3}$	10.4	$1.027 \pm 2.36 \times 10^{-3}$
40.3	$0.740 \pm 7.39 \times 10^{-4}$	42.5	$1.290 \pm 2.69 \times 10^{-3}$	14.9	$1.773 \pm 2.65 \times 10^{-2}$				
49.3	$0.702 \pm 7.84 \times 10^{-4}$	53.7	$1.399 \pm 5.98 \times 10^{-3}$	15.6	$1.719 \pm 1.89 \times 10^{-2}$				
59.7	$0.664 \pm 7.30 \times 10^{-4}$	64.2	$1.485 \pm 1.41 \times 10^{-3}$						
70.2	$0.627 \pm 1.46 \times 10^{-3}$	74.6	$1.514 \pm 2.22 \times 10^{-2}$						
80.6	$0.593 \pm 4.79 \times 10^{-4}$	80.6	$1.692 \pm 1.73 \times 10^{-2}$						
85.0	$0.572 \pm 1.07 \times 10^{-3}$	85.0	$1.723 \pm 4.61 \times 10^{-2}$						

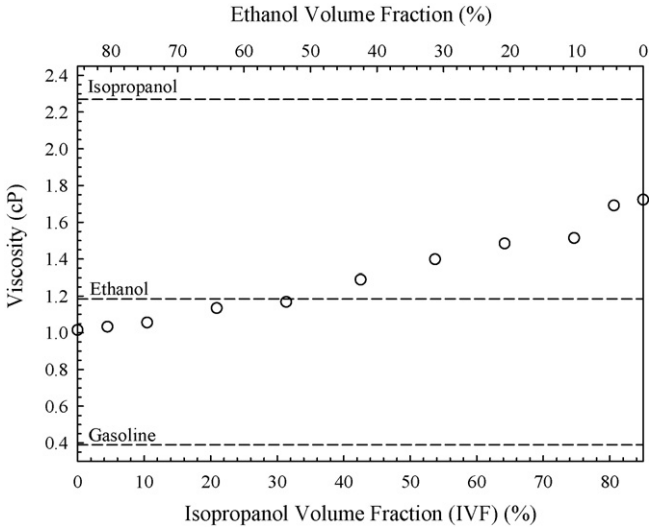

Fig. 4. Observed viscosity variations for fuel blends comprising of 15% gasoline and various volume fractions of ethanol and isopropanol.

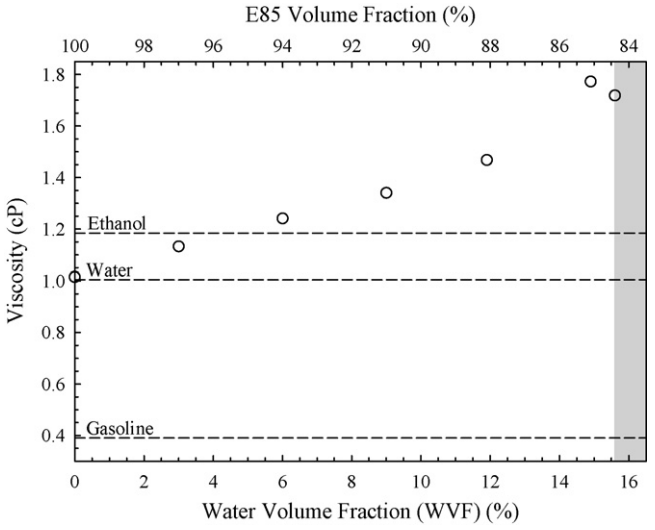

Fig. 5. Observed viscosity variations for mixtures of the E85 fuel with various volume fractions of water.

ment, the water volume fraction is increased by a few percentage points and the experiments are repeated until two distinctive separate liquid phases can be visually detected in the glass tube. Once phase separation is detected, additional experiments are conducted to obtain a more exact threshold water volume fraction for phase separation. It should be noted that for this and all subsequent experiment sets, viscosity experiments are conducted only when the resulting alcohol–gasoline–water mixture is a single-phase liquid. Determination of viscosity variations of each liquid phase in a two-phase liquid–liquid system is beyond the scope of this study. Emulsion of the solution, which is given by a white cloudy appearance of the mixture, is detected near the phase separation threshold water volume fraction for this and all subsequent experiments. When emulsion occurs, the liquid mixture gives the appearance of a single-phase liquid, but addition of more water will cause the mixture to partition into two separate liquids. It is interesting to note that emulsion of the mixture actually caused a decrease in the observed viscosity trend. This phenomenon is observed for this and all subsequent experiment sets.

The experimentally derived averaged viscosity values for this set of experiments are listed in Table 2 and plotted as circles in Fig. 5. This figure shows that as more water is added to the E85 fuel, the viscosity of the resulting mixture increases steadily, despite the fact that the viscosity of water is relatively lower as compared against the viscosity of ethanol. For subsurface contaminant transport analysis, this increase in viscosity will cause a decrease in the liquid contaminant downward velocity through the unsaturated zone as the mixture encounters water. Emulsion of the mixture is detected at a water volume fraction of approximately 15.6%. Note the slight decrease in the observed viscosity at this water volume fraction. At water volume fractions greater than 15.6%, the solution partitions itself into a two-phase liquid–liquid system as indicated by the shady area in the figure.

3.5. Mixtures of the M85 fuel with various volume fractions of water

The forth set of experiments is conducted to determine viscosity variations for liquid mixtures comprising of the M85 fuel with various volume fractions of water. The experimental procedure is identical to the procedure described in the previous section. The experimentally derived averaged viscosity values are listed in Table 2 and plotted as circles in Fig. 6. It is determined that at water volume fractions greater than 7.5%, the solution partitions to a two-phase liquid–liquid system as indicated by the shady area in the figure. Note that the phase separation threshold water volume fraction is considerably lower for the M85 fuel as compared against the E85 fuel. The work by Lee and Peters [7] shows that the two-phase region in a ternary phase diagram for methanol is considerably larger than for ethanol when mixed with water and nonaqueous phase liquids other than gasoline, which indicates that less water is required for a solution-containing methanol to partition into a two-phase system. Again, as the water volume fraction increases, the viscosity increases and a decrease in viscosity is observed when emulsion of the solution is detected.

3.6. Mixtures of a novel fuel blend with various volume fractions of water

The fifth set of experiments is conducted to determine viscosity variations for liquid mixtures comprising of an unique high-alcohol content fuel blend with various volume fractions of water. The fuel

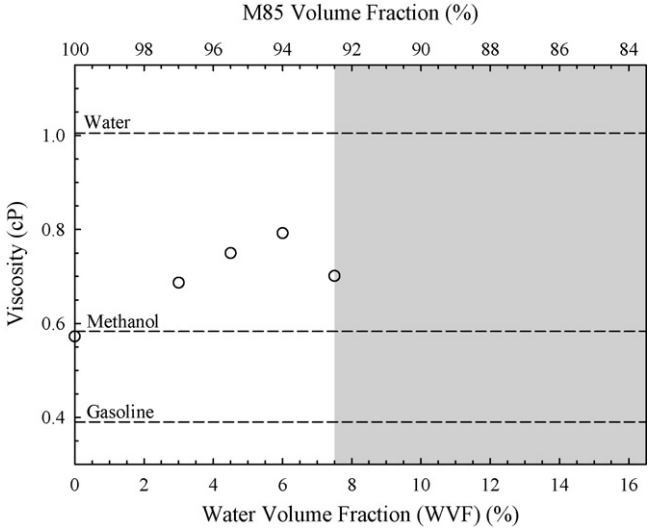

Fig. 6. Observed viscosity variations for mixtures of the M85 fuel with various volume fractions of water.

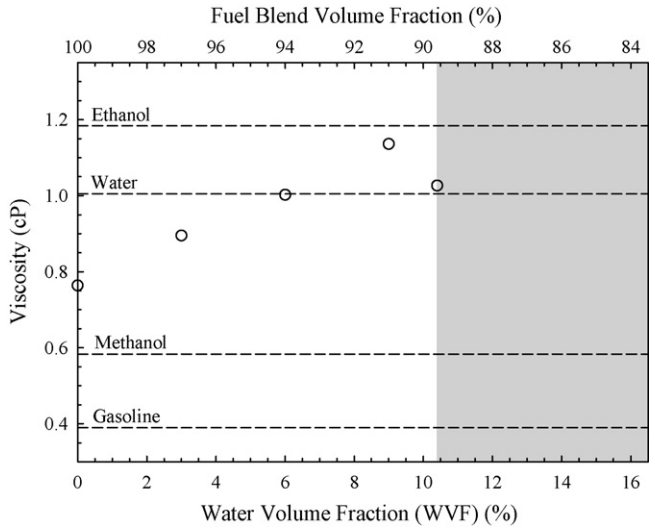

Fig. 7. Observed viscosity variations for mixtures of a unique high-alcohol content fuel blend with various volume fractions of water.

blend contains 15% gasoline, 42.5% ethanol, and 42.5% methanol. This mixture can be a possible fuel blend to alleviate the ethanol demand. Again, the experimental procedure is identical to the procedure described previously. The experimentally derived averaged viscosity values are listed in Table 2 and plotted as circles in Fig. 7. It is determined that at water volume fractions greater than 10.4%, the solution partitions to a two-phase liquid–liquid system as indicated by the shady area in the figure. Note that the phase separation threshold water volume fraction for this fuel blend is lower than the threshold value for the E85 fuel, but higher than the value for the M85 fuel.

4. Summary

In this research, five sets of experiments were conducted to determine viscosity variations of various high-alcohol content gasoline fuel blends and high-alcohol content fuel blends mixed with water. A commercially available falling-ball viscometer was used to determine the viscosity of each mixture. The viscometer was modified by adding an additional relatively small metal spherical ball inside the glass tube before insertion of the stainless steel falling ball. The metal ball can be moved vertically upward and downward via an external moving magnet. Movement of the metal ball allowed mixing of the liquids and repeated falling ball time-of-descent observations of the same solution. A unique leveling apparatus was designed and constructed to hold the viscometer in an exact vertical position.

For the first set of experiments, where the mixtures were blends of 15% gasoline and various volume fractions of ethanol and methanol, it was observed that the solution viscosity decreased steadily as the methanol volume fraction increased. For the second set of experiments, where the mixtures were blends of 15% gasoline and various volume fractions of ethanol and isopropanol, it was observed that the solution viscosity increased as the isopropanol volume fraction increased. For the next three sets of experiments, water was added to the high-alcohol content gasoline fuel blends and viscosity variations were determined. For all alcohol–gasoline–water mixtures considered in this study, the observed solution viscosity increased with increasing water volume fraction until emulsion of the solution was detected, at which point the observed viscosity decreased. The experimentally derived liquid viscosity variations presented in this study should be incorporated into mathematical models for a more accurate prediction on the movement of these liquid contaminants through the subsurface.

Acknowledgement

This research was partially funded by a grant from the West Virginia NASA Space Grant Consortium.

References

[1] California Energy Commission, Methanol as a Transportation Fuel. Retrieved from http://www.energy.ca.gov/afvs/vehicle_fact_sheets/methanol.html.
[2] S. Feng, A.L. Graham, J. Abbott, L. Mondy, Improving falling ball tests for viscosity determination, J. Fluid Eng. 128 (2006) 157–163.
[3] C.W. Fetter, Contaminant Hydrogeology, 2nd edition, Prentice-Hall, New Jersey, USA, 1999.
[4] Handbook for Handling, Storing, and Dispensing E85, prepared by the National Renewable Energy Laboratory (NREL), a Department of Energy National Laboratory, 2006.
[5] A. Kumagai, C. Yokoyama, Liquid viscosity of binary mixtures of methanol with ethanol and 1-propanol from 273.15 to 333.15 K, Int. J. Thermophys. 19 (1) (1998) 3–13.
[6] K.Y. Lee, Phase partitioning modeling of ethanol, isopropanol, and methanol with BTEX compounds in water, Environ. Pollut. 154 (2008) 320–329.
[7] K.Y. Lee, C.A. Peters, UNIFAC modeling of cosolvent phase partitioning in non-aqueous phase liquid–water systems, J. Environ. Eng. ASCE 130 (4) (2004) 478–483.
[8] L.W. Mays, Water Resources Engineering, John Wiley & Sons Inc., New Jersey, USA, 2001.